

Research article

Open Access

Effect of phospholipase A₂ inhibitory peptide on inflammatory arthritis in a TNF transgenic mouse model: a time-course ultrastructural studyMaung-Maung Thwin¹, Eleni Douni², Vassilis Aidinis², George Kollias², Kyoko Kodama³, Kazuki Sato³, Ramapatna L Satish⁴, Ratha Mahendran⁴ and Ponnampalam Gopalakrishnakone¹¹Venom & Toxin Research Program, Department of Anatomy, National University of Singapore, Singapore²Institute of Immunology, Biomedical Sciences Research Center, Al Fleming, 34 Al Fleming Street, 16672 Vari, Greece³Fukuoka Women's University, Fukuoka 813-8529, Japan⁴Department of Surgery, Faculty of Medicine, National University of Singapore, SingaporeCorresponding author: Ponnampalam Gopalakrishnakone, antgopal@nus.edu.sg

Received: 19 Jan 2004 Revisions requested: 6 Feb 2004 Revisions received: 12 Mar 2004 Accepted: 25 Mar 2004 Published: 28 Apr 2004

Arthritis Res Ther 2004, **6**:R282-R294 (DOI 10.1186/ar1179)© 2004 Thwin *et al.*; licensee BioMed Central Ltd. This is an Open Access article: verbatim copying and redistribution of this article are permitted in all media for any purpose, provided this notice is preserved along with the article's original URL.**Abstract**

We evaluated the therapeutic effect of secretory phospholipase A₂ (sPLA₂)-inhibitory peptide at a cellular level on joint erosion, cartilage destruction, and synovitis in the human tumor necrosis factor (TNF) transgenic mouse model of arthritis. Tg197 mice ($N = 18$) or wild-type ($N = 10$) mice at 4 weeks of age were given intraperitoneal doses (7.5 mg/kg) of a selective sPLA₂ inhibitory peptide, P-NT.II, or a scrambled P-NT.II (negative control), three times a week for 4 weeks. Untreated Tg197 mice ($N = 10$) were included as controls. Pathogenesis was monitored weekly for 4 weeks by use of an arthritis score and histologic examinations. Histopathologic analysis revealed a significant reduction after P-NT.II treatment in synovitis, bone erosion, and cartilage destruction in particular. Conspicuous ultrastructural alterations seen in articular chondrocytes (vacuolated cytoplasm and loss of nuclei) and synoviocytes (disintegrating nuclei and vacuoles,

synovial adhesions) of untreated or scrambled-P-NT.II-treated Tg197 mice were absent in the P-NT.II-treated Tg197 group. Histologic scoring and ultrastructural evidence suggest that the chondrocyte appears to be the target cell mainly protected by the peptide during arthritis progression in the TNF transgenic mouse model. This is the first time ultrastructural evaluation of this model has been presented. High levels of circulating sPLA₂ detected in untreated Tg197 mice at age 8 weeks of age were reduced to basal levels by the peptide treatment. Attenuation of lipopolysaccharide- and TNF-induced release of prostaglandin E₂ from cultured macrophage cells by P-NT.II suggests that the peptide may influence the prostaglandin-mediated inflammatory response in rheumatoid arthritis by limiting the bioavailability of arachidonic acid through sPLA₂ inhibition.

Keywords: peptide, secretory phospholipase A₂ inhibition, rheumatoid arthritis, TNF transgenic mouse model, ultrastructural alterations**Introduction**

Secretory phospholipase A₂ (sPLA₂) is a key enzyme in the production of diverse mediators of inflammatory and related conditions [1]. Because of the crucial role it plays in inflammatory diseases such as rheumatoid arthritis (RA) [2], sPLA₂ is referred to as inflammatory PLA₂ [3]. High levels of sPLA₂ have been found in synovial tissues and fluid from patients with RA [2,4]. Purified synovial PLA₂ can elicit an inflammatory arthritogenic response when injected into the joint space of healthy rabbits and rats [5,6]. It has been

reported that sPLA₂ expression parallels the severity of the inflammatory process with lack of enhancement of cytosolic phospholipase A₂ (cPLA₂) mRNA in an adjuvant arthritis model, thus indicating the pathogenic role played by sPLA₂ [7]. Colocalization studies using primary synovial fibroblasts from RA patients have also suggested sPLA₂ as a critical modulator of cytokine-mediated synovial inflammation in RA [8]. As a result of its important role in the inflammatory response, inhibition of sPLA₂ is a target for the treatment of inflammatory diseases. Inhibition of sPLA₂

AA = arachidonic acid; ANOVA = analysis of variance; AS = arthritis score; cPLA₂ = cytosolic phospholipase A₂; DMSO = dimethyl sulfoxide; HS = histopathologic score; LPS = lipopolysaccharide; PGE = prostaglandin E; PIP = phospholipase inhibitor from python; RA = rheumatoid arthritis; r-ER = rough endoplasmic reticulum; SEM = standard error of the mean; sPLA₂ = secretory phospholipase A₂; Tg = transgenic; TNF = tumor necrosis factor.

could result in suppression of several classes of proinflammatory lipids such as prostaglandins, leukotrienes, platelet-activating factor, and lysophospholipid [1].

Elevated levels of circulating sPLA₂ are usually associated with high blood levels of proinflammatory cytokines [9], which are used as an indicator of the extent of systemic inflammation [10,11]. sPLA₂ has been shown to activate the production of proinflammatory cytokines in blood and synovial fluid monocytes [12], suggesting that the two can cooperate to promote inflammation by enhancing each other's secretion. sPLA₂ may act on the cells stimulated with such cytokines, leading to augmentation of the inflammatory responses. The fact that cotransgenic sPLA₂ and tumor necrosis factor α (TNF- α) mice show more extensive swelling than TNF- α transgenic mice [13] may be evidence in support of a possible synergism between sPLA₂ and TNF. Hence, inhibition of sPLA₂ may further help to suppress inflammation in RA by blocking the formation of proinflammatory cytokines.

A significant reduction of the inflammatory response has been reported in animals injected with natural or synthetic sPLA₂ inhibitors [14,15]. Two families of endogenous proteins, namely lipocortins and uteroglobin, have been shown to possess anti-inflammatory properties due to their ability to inhibit sPLA₂. Synthetic peptides called antiflammins derived from these proteins are one of the most potent classes of anti-inflammatory agents identified to date [16]. A recombinant protein termed PIP (phospholipase inhibitor from python), which we have expressed from the liver of a nonvenomous snake, *Python reticulatus* [17], exhibits *in vivo* anti-inflammatory activity that correlates well with its *in vitro* inhibitory potency towards sPLA₂. In a clinically relevant model of postsurgical peritoneal adhesion, the peptide analog P-PB.III, which has a fragment of an anti-inflammatory protein PIP included in its sequence, exhibits stronger *in vivo* anti-inflammatory activity than that displayed by anti-flammin [18]. Further screening of the PIP amino acid sequence provides us with a new peptide with improved potency. This new 17-mer peptide ⁵⁶LGRVDIHVWDGVYIRGR⁷² is a selective inhibitor of human sPLA₂-IIA, with an amino acid sequence corresponding to residues 56–72 of the native protein PIP. It significantly reduces high levels of sPLA₂ detected in rat hippocampal homogenates after intracerebroventricular injections of a neurotoxin, kainic acid [19]. These findings establish that peptides or recombinant proteins that inhibit sPLA₂, or their peptide derivatives, are highly attractive candidates for clinical development as anti-inflammatory agents.

The present study was designed to investigate the effect of a selective sPLA₂-inhibitory peptide, P-NT.II, on ultrastructural changes of ankle-joint synovitis, cartilage degradation,

and bone erosion in the Tg197 TNF transgenic mouse model of arthritis [20], and to assess the effects of peptide intervention on the clinical and histologic indices of RA.

Materials and methods

Animals

The generation and characterization of Tg197 human TNF transgenic mice have been previously described [20]. Tg197 mice generated on CBA \times C57BL/6 genetic backgrounds and littermate controls were bred and maintained at the animal facilities of the Biomedical Sciences Research Center, Alexander Fleming, Athens, Greece, under specific-pathogen-free conditions. All of the Tg197 mice typically developed polyarthritis 3–4 weeks after birth, whereas nontransgenic (wild-type) mice remained normal. Mice were given conventional oral food and water *ad libitum*. All procedures involving animals were in compliance with the Declaration of Helsinki principles.

Experimental protocol

A total of 44 weight-matched mice (34 Tg197 and 10 non-transgenic wild-type littermates) were divided into six groups for subsequent gross observations and histopathologic analyses – untreated Tg197 group ($N = 10$), P-NT.II-treated Tg197 group ($N = 18$), scrambled-P-NT.II-treated Tg197 group ($N = 6$), P-NT.II-treated wild-type group ($N = 4$), scrambled-P-NT.II-treated wild-type group ($N = 4$), and Tg197 baseline group – just before the treatment at 4 weeks of age ($N = 4$). Nontransgenic mice were given the same dose of P-NT.II or scrambled P-NT.II, and the same regimen of treatment, as the Tg197 mice.

Peptide synthesis and administration

P-NT.II (test peptide) and the scrambled P-NT.II (negative control peptide) were synthesized using the solid-phase method with 9-fluorenylmethoxy carbonyl chemistry and were purified and validated as described elsewhere [18]. They were stored lyophilized at -20°C in sealed tubes and were dissolved freshly before use in 0.1% dimethyl sulfoxide (DMSO). Each Tg197 or wild-type mouse was given intraperitoneal injections of P-NT.II or the scrambled P-NT.II (7.5 mg/kg) in 50 μl of vehicle (0.1% final DMSO concentration), three times a week for 4 weeks (i.e. from age 4–8 weeks).

Clinical assessment

This was done by gross observations based on body-weight measurements and arthritis scoring, which were done twice weekly from 4 weeks (baseline) to 8 weeks of age (end of the study), after which all the animals were killed by CO₂ inhalation. The level of severity of clinical arthritis was evaluated based on an arthritis score (AS) taken on both ankle joints. Average scores on a scale of 0–3 were used; 1 = mild arthritis (joint swelling); 2 = moderate arthritis (severe joint swelling and deformation, no grip

strength); 3 = severe arthritis (ankylosis detected on flexion, and severely impaired movement) [21].

Histologic examinations

The whole ankle joints harvested from the right side of each mouse were fixed overnight in 10% formalin, decalcified in 30% citrate-buffered formic acid for 3 days at 4°C, dehydrated in a graded series of methanol and xylene, and then embedded in paraffin. Thin sections (6 µm thick) were stained with hematoxylin and eosin, and histopathologic scorings performed under the light microscope (Leitz Aristoplan) by a blinded observer. The histopathologic score (HS) was evaluated [21] using a scale of severity ranging from 1 to 4, where 1 = hyperplasia of the synovial membrane and presence of polymorphonuclear infiltrates, 2 = pannus and fibrous tissue formation and focal subchondral bone erosion, 3 = articular cartilage destruction and bone erosion, and 4 = extensive articular cartilage destruction and bone erosion.

Scoring of joint parameters

Arbitrary scores were used to assess the extent of synovitis, cartilage destruction, and bone erosion. Semiquantitative scores from 0 to 4 were used for each histopathologic parameter [22]. Synovitis: 0 = normal; 1 = mild synovial hypertrophy (<5 cell layers) with few inflammatory cells; 2 = moderate synovial hypertrophy (<20 cell layers) with accumulation of inflammatory cells into intrasynovial cysts; 3 = pannus and fibrous tissue formation; and 4 = pannus and fibrous tissue formation on both sides of the ankle joint. Cartilage damage: 0 = intact; 1 = minor (<10%); 2 = moderate (10–50%); 3 = high (50–80%); and 4 = severe (80–100%). Bone erosions: 0 = normal; 1 = mild (focal subchondral erosion); 2 = moderate (multiple subchondral erosions); 3 = high (as above + focal erosion of talus); and 4 = maximum (multiple erosions of tarsal and metatarsal bones).

Transmission electron microscopy

Ankle joints dissected from the left hind leg of each mouse were split open longitudinally through the midline between the tibia and the talus, prefixed overnight with 2.5% glutaraldehyde in phosphate buffer, pH 7.4, and rinsed with the buffer. After they had been postfixed with 1% osmium tetroxide in phosphate buffer for 2 hours, they were dehydrated in a graded series of ethanol and embedded in epoxy resin (Araldite). Semithin sections (1.0 µm) were cut and stained with methylene blue to reveal their orientation for ultrathin sectioning and for histopathologic scoring under the light microscope. Ultrathin sections (80–90 nm) were then cut with an ultramicrotome (Ultracut E; Riechert-Jung, Leica, Vienna, Austria), mounted on copper grids, counterstained with uranyl acetate and lead citrate, and evaluated in the electron microscope (CM120 Biotwin; FEI Company, Electron Optics, Eindhoven, The Netherlands).

Measurement of serum PLA₂

sPLA₂ was measured in the serum of transgenic (Tg197) mice and nontransgenic wild-type controls, using an *Escherichia coli* membrane assay as described previously [18]. In brief, [³H]arachidonate-labeled *E. coli* membrane suspension (5.8 µCi/µmol, PerkinElmer Life Sciences, Inc, Boston, MA, USA) was used as substrate, and 25 mM CaCl₂-100 mM Tris/HCl (pH 7.5) as assay buffer. The reaction mixture, containing substrate (20 µl) and either purified human synovial sPLA₂ standard (1–80 ng/ml; Cayman Chemical Company, Ann Arbor, MI, USA) or serum (10 µl), in a final volume of 250 µl in assay buffer, was incubated at 37°C for 1 hour, and the reaction was terminated with 750 µl of chilled phosphate-buffered saline containing 1% bovine serum albumin. Aliquots (500 µl) of the supernatant were then taken, for measurement of the amount of [³H]arachidonate released from the *E. coli* membrane using liquid scintillation counting (LS 6500 Scintillation Counter; Beckman Inc., Fullerton, CA, USA). The amount of sPLA₂ present in the serum was calculated from the standard curve and is expressed as ng/ml ± SEM.

Cell culture

The murine macrophage cell line J774 (American Type Culture Collection, Manassas, VA, USA) was cultured at 37°C in humidified 5% CO₂/95% air in Dulbecco's modified Eagle's medium containing 10% fetal bovine serum, 2 mM glutamine, 20 mM HEPES, 100 IU/ml penicillin, and 100 µg/ml streptomycin. After growing to confluence, the cells were dislodged by scraping, plated in 12 culture wells at a density of 5 × 10⁵ cells/ml per well, and allowed to adhere for 2 hours. Thereafter, the medium was replaced with fresh medium containing lipopolysaccharide (LPS) (2 µg/ml) and one of the PLA₂ inhibitors (P-NT.II, scrambled P-NT.II, or LY315920 [Lilly Research Laboratories, Indianapolis, IN, USA], dissolved in DMSO [final concentration 0.1% v/v]). Peptides were tested at various concentrations ranging from 0.01 to 40 µM. After incubation in 5% CO₂/95% air at 37°C for 20 hours, culture medium supernatants were collected and stored frozen (-80°C) until use. In parallel experiments, cells were stimulated with mouse recombinant TNF (10 ng/ml; Sigma, St. Louis, MO, USA) for 20 hours, in the presence or absence of 10 µM P-NT.II or LY315920 dissolved in DMSO (0.1% final concentration). Culture medium supernatants were collected after centrifugation (10,000 g, 4°C, 15 min) and stored at -80°C prior to measurement of prostaglandin E₂ (PGE₂).

Cell viability assays

XTT (sodium 3'-[(phenyl amine carboxyl)-3,4-tetrazolium]-bis(4-methoxy-nitro) benzene sulfonic acid hydrate) Cell Proliferation Kit II (Roche Applied Science) was used to assess the possible cytotoxic effect of the peptide P-NT.II on the mouse macrophage J774 cell line.

Measurement of PGE₂

PGE₂ (EIA kit-monoclonal; Cayman) concentrations were measured in the cell-culture supernatants in accordance with the manufacturer's instructions.

Statistical analysis

Statistical analyses were performed using GraphPad Prism software to calculate the means and SEMs. Group means were compared by using one-way analysis of variance (ANOVA), followed by Bonferroni's multiple comparison post test to identify statistically significant differences (i.e. $P < 0.05$).

Results

Gross histologic findings

Figure 1 shows the histologic features of ankle joints of Tg197 mice in the untreated, P-NT.II-treated, and scrambled-P-NT.II-treated groups. Gross histologic findings of the three experimental groups are summarized in Table 1. At 8 weeks of age, ankle joints from the untreated Tg197 group were moderately (90% with HS 3) to severely (10% with HS 4) damaged, with pannus and fibrous tissue formation and focal subchondral bone erosion. Articular cartilage destruction and bone erosion were observed in 90% of those joints (Fig. 1a,1b). In contrast, all the articular cartilage surfaces and associated synovial linings of the ankle joints of the P-NT.II-treated group at 2 weeks post-treatment (i.e. age 6 weeks) were only mildly affected (HS 2), with no evidence of cartilage or bone erosion (Fig. 1c), and 25% of joints were affected moderately (HS 3) at 4 weeks post-treatment (i.e. age 8 weeks) (Fig. 1d). In contrast, 83.3% of joints of scrambled-P-NT.II-treated Tg197 mice at 8 weeks of age were moderately damaged (HS 3) (Fig. 1e,1f), with histologic features similar to those of the untreated Tg197 mice. Although the disease, as assessed by the HS, was significantly lower in the P-NT.II-treated group than in the untreated or scrambled-P-NT.II-treated groups, visual disease scores (ASs) did not correlate well with the HS. In contrast to HSs, ASs of mice treated with P-NT.II did not significantly differ from those of the untreated or scrambled-P-NT.II-treated group (Fig. 2).

Analytical HS

To assess specific effects of the peptide P-NT.II on synovitis, cartilage destruction, and bone erosion, we conducted a semiquantitative scoring analysis for each of these pathologic parameters. P-NT.II treatment in Tg197 mice resulted in a significant reduction ($P < 0.05$) in all three analytical HSs as compared with those of untreated or scrambled-P-NT.II-treated Tg197 mice, which all developed synovitis with severe articular cartilage degradation and bone erosions (Fig. 3). Statistical analysis revealed a greater beneficial effect of P-NT.II on cartilage destruction and bone erosion ($**P < 0.01$ versus untreated or scrambled-P-NT.II-treated groups for both parameters) than on

synovitis ($*P < 0.05$ versus untreated or scrambled-P-NT.II-treated groups).

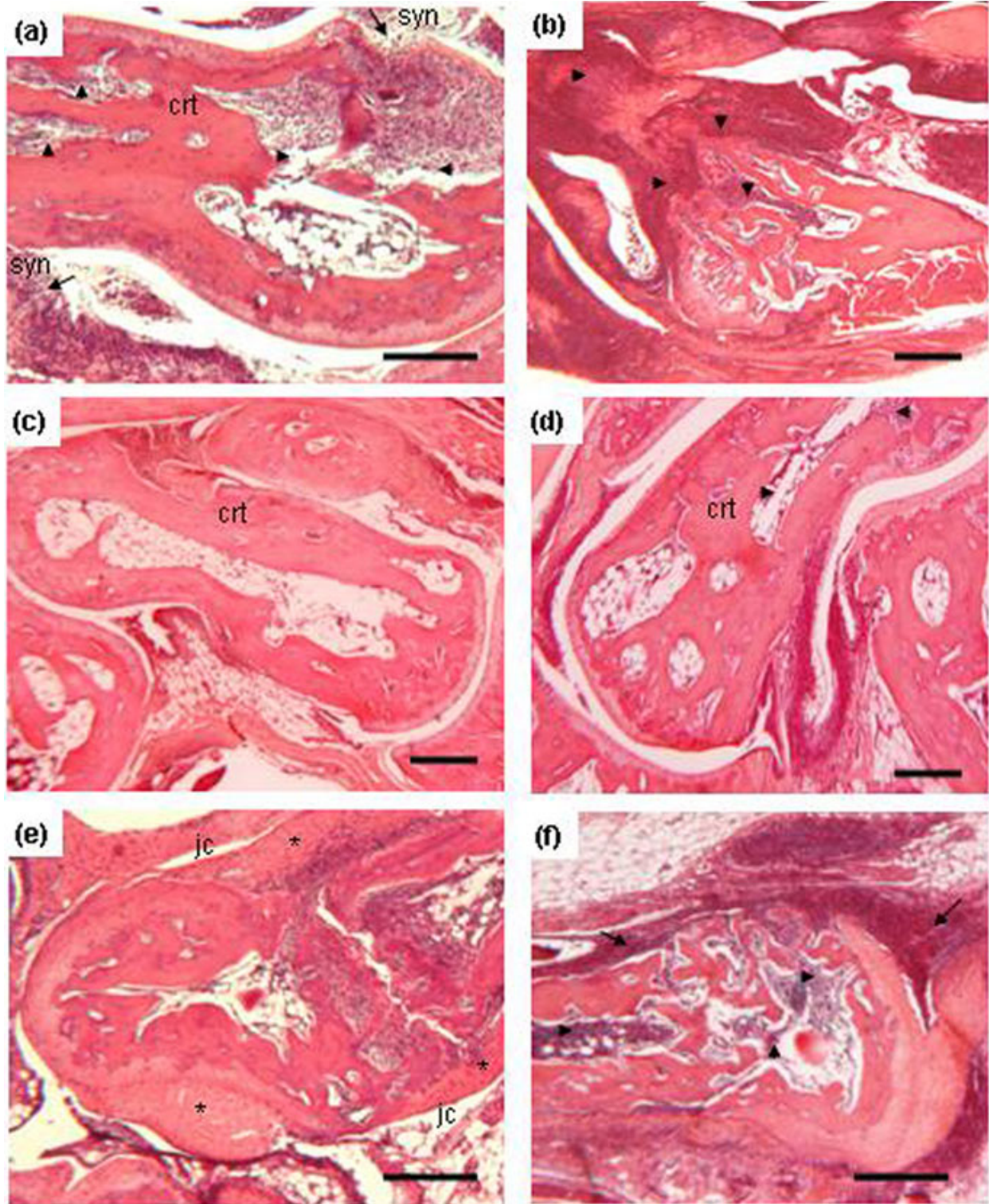
Ultrastructural changes in articular cartilage

Articular cartilage in the ankle joints of all untreated Tg197 mice was generally damaged at 8 weeks of age (Fig. 4c,4d,4e,4f) as compared with normal morphology seen in control, wild-type mice (Fig. 4a). No significant ultrastructural changes in the nucleus and plasma membrane were noted at the cellular level in the articular cartilage of untreated Tg197 mice at age 4 weeks (baseline) except for some minor changes including vacuoles, dilated cisternae, and the presence of granular materials seen inside the cytoplasm (Fig. 4b). In the 8-week-old mice, the chondrocytes on the surface of the superficial cartilage layer had become necrotic, with alterations of cartilage developed in most cases (Fig. 4c,4d,4e,4f). The cell body and nucleus of some chondrocytes became large and rounded, resulting in vacuolation, and the cytoplasm was transparent, with an accumulation of intracytoplasmic filaments (Fig. 4c). Degenerating chondrocytes with greatly vacuolated cytoplasm and pyknotic nuclei (Fig. 4d), and chondrocytes with complete loss of nuclei and disrupted rough endoplasmic reticulum (r-ER) (Fig. 4e,4f), were also observed. In contrast, the ultrastructural features of chondrocytes 1–4 weeks after P-NT.II treatment (i.e. age 5–8 weeks; Fig. 5a) did not substantially differ from those seen in the joints of normal wild-type mice (Fig. 4a). Most of them had a prominent nucleus, lined by plasma membrane with short cytoplasmic protrusions, and vacuoles, r-ER, and mitochondria in the cytoplasm. The ultrastructure of chondrocytes of the scrambled-P-NT.II-treated joints at 8 weeks of age (Fig. 5b) were more or less similar to those described for untreated Tg197 mice with degenerating features such as the greatly vacuolated cytoplasm and pyknotic nuclei (cf. Fig. 4d) or loss of nucleus, disrupted r-ER (cf. Fig. 4f), and swollen mitochondria with distorted cristae (cf. Fig. 4c).

Ultrastructural changes in synovium

The early response of the synovial membrane in the untreated Tg197 mice at age 4 weeks (baseline) was synovial hyperplasia, with the presence of type A and B synovial cells along with inflammatory cells such as lymphocytes, macrophages, and mast cells. Type A cells were similar to macrophage cells and were characterized by many vesicles, vacuoles, and a higher number of cell processes. Type B cells were similar to fibroblast cells and contained small vesicles and r-ER. The later response (at ≥ 5 weeks of age) included degeneration of synovial cells, with swollen mitochondria and cell fragmentations. In areas of high inflammation, the synovial tissue (mostly type A cells) had proliferated into the articular cavity (Fig. 6a). Type A and B cells in the synovium were no longer distinguishable at age 6 weeks and thereafter. The synovial membrane was lined by closely packed elongated synoviocytes which

Figure 1



Histologic findings in the ankle joints of Tg197 mice. **(a,b)** Untreated mice: (a) partially altered articular cartilage (crt) with bone erosion (arrowhead), and presence of inflammatory infiltrates (arrow) in the synovial (syn) tissue; (b) extensive articular cartilage destruction and bone erosion (arrowhead). **(c,d)** P-NT.II-treated mice: (c) minor cartilage changes (crt) with absence of bone erosion; (d) focal articular cartilage destruction (crt) and minor bone erosion (arrowhead). **(e,f)** Mice treated with scrambled P-NT.II: (e) the joint cavity (jc) is lined with synovitis (*); (f) cartilage destruction and bone erosion (arrowhead) are present, along with inflammatory infiltrates (arrow). Nontransgenic controls showed normal joint structures throughout the study (data not shown). (Hematoxylin & eosin staining; original magnification $\times 25$ in a, e, f; $\times 10$ in b, c, d. Bars = 500 μm).

Table 1**Histopathologic assessment of ankle joints**

Treatment	Time course (weeks)	Joints scored	% of total at indicated HS			
			HS 2	HS 3	HS 4	HS (Mean \pm SEM)
None	4	10	0	90.0	10	3.30 \pm 0.11 ^a
P-NT.II*	1	4	100	0	0	2.12 \pm 0.12
P-NT.II*	2	4	100	0	0	2.37 \pm 0.12
P-NT.II*	3	4	75	25	0	2.50 \pm 0.20
P-NT.II*	4	4	75	25	0	2.62 \pm 0.31 ^b
Scrambled-P-NT.II-treated (negative control peptide)	4	6	16.7	83.3	0	3.25 \pm 0.17 ^c

*Tg197 mice injected (intraperitoneally) with the test peptide P-NT.II were killed at weekly intervals ($N = 4$ per group) for 4 weeks and their ankle joints examined. For untreated and negative control groups, ankle joints were harvested only at the end of the 4 weeks' study course for one-time examination. Histologic scoring was performed semiquantitatively by a blinded examiner. HS 2 = pannus and fibrous tissue formation and focal erosion of subchondral bone; HS 3 = articular cartilage destruction and bone erosion; HS 4 = extensive articular cartilage destruction and bone erosion. *a* versus *b*, *b* versus *c* = significantly different ($P < 0.05$; one-way analysis of variance with Bonferroni's multiple comparison test). HS, histopathologic score; SEM, standard error of the mean.

were sealed by junctional systems of the adherent type (Fig. 6b). Large amounts of fibrin deposition on the synovial surface could be seen, and the two opposing, flattened synoviocytes with fibrin between them indicated the existence of synovial adhesion (Fig. 6d). Also, degenerating synoviocytes with disintegrating nuclei and vacuolated cytoplasm were randomly seen in the synovium (Fig. 6c). Synoviocytes appeared flattened, and partially degranulated mast cells were seen under the synovium (Fig. 6e).

P-NT.II treatment tended to decrease the number of inflammatory cells, with less degeneration of synovial cells and cell fragmentation seen in the joints of the treated group (Fig. 7b). The peptide P-NT.II retained at least the basic structural organization of the synovial membrane seen in the control wild-type mice (Fig. 7a), while the synoviocytes from mice treated with scrambled P-NT.II (Fig. 7c) were structurally indistinguishable from those seen in untreated joints (cf. Fig. 6). In those joints, the synovial cells were seen lining up close together, and many cell fragments resulting from degenerating cells were present in the synovium, along with infiltrating mast cells (Fig. 7c).

Serum levels of sPLA₂

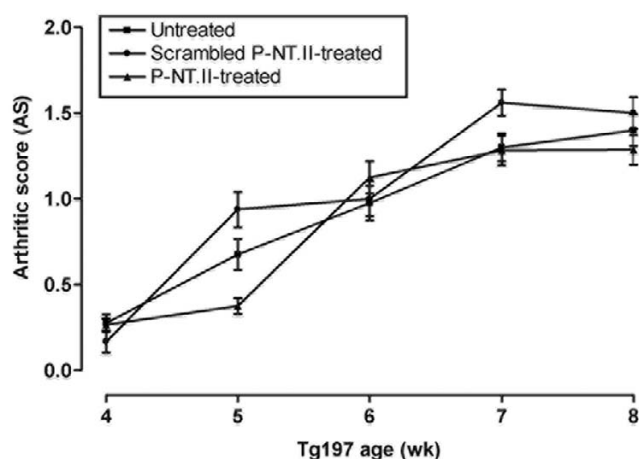
In a time-course study to evaluate the specific effect of peptide in modulating the serum sPLA₂ levels in Tg197 mice (Fig. 8), P-NT.II significantly suppressed the circulating sPLA₂ in the mice at age 8 weeks ($P < 0.05$), by comparison with the serum levels of the untreated mice of same age. In contrast, the circulating sPLA₂ of scrambled-P-NT.II-treated and untreated Tg197 mice at age 8 weeks were not significantly different ($P > 0.05$), thus indicating the specific effect of the peptide P-NT.II on sPLA₂ levels.

PGE₂ release from cultured macrophages

The suppressive effect of P-NT.II and sPLA₂-selective inhibitor LY315920 (Lilly) on LPS- and TNF-stimulated PGE₂ production was examined in mouse macrophage cell cultures (Fig. 9). Production of PGE₂ in the medium increased approximately sixfold from the basal level of 55 ± 6 pg/ml to 320 ± 35 and 330 ± 11 pg/ml (mean \pm SD, $N = 5$), after 20 hours' stimulation of cultured cells with LPS (2 μ g/ml) (Fig. 9a) or TNF (10 ng/ml) (Fig. 9b), respectively. When the inhibitors were coincubated with either LPS- or TNF-stimulated macrophages in the medium, both P-NT.II and LY315920 (final concentration 10 μ M) dose-dependently inhibited PGE₂ production, with estimated IC₅₀ values of 25 and 30 μ M, respectively. In contrast, scrambled P-NT.II (negative control) showed no inhibitory effect on either LPS- or TNF-induced PGE₂ release in the culture medium. Neither the peptide nor LY315920 affected the cellular viability, when tested by XTT assay kit at the highest concentration (40 μ M) used in culture experiments ($E_{492\text{ nm}}$ values of 0.89 ± 0.02 , 0.84 ± 0.021 , and 0.92 ± 0.019 for untreated, P-NT.II-treated, and LY315920-treated cells, respectively).

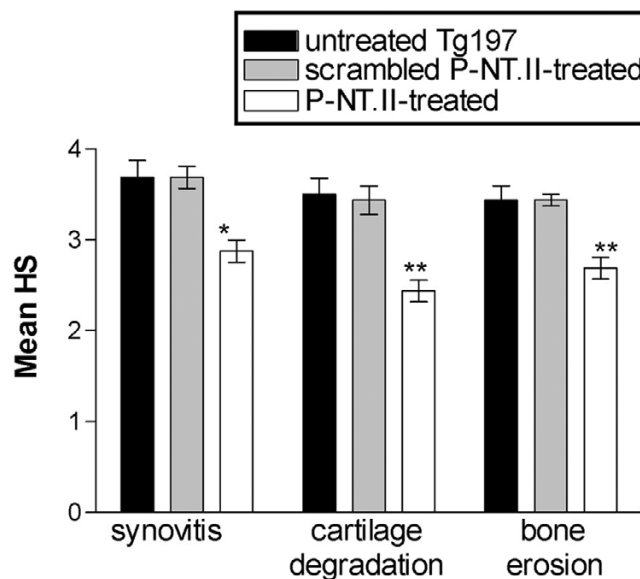
Discussion

Here we report the beneficial effect of peptide treatment, and the ultrastructural changes seen at the cellular level in the articular cartilage and synovium of the ankle joints of TNF transgenic Tg197 mice treated with the anti-inflammatory peptide P-NT.II. While several studies have previously been carried out on the early ultrastructural changes in other animal models of experimental arthritis [23-25], no morphological evaluations in this TNF transgenic mouse model of RA have yet been available, in either the absence or the presence of therapeutic intervention.

Figure 2

The arthritis score (AS) in Tg197 mice changes with time course. The AS was determined on both ankle joints of each mouse by a blinded examiner, using a scale of 0–3 as described in Materials and methods. Values are the mean \pm SEM.

The lesions in the TNF transgenic mouse model of arthritis we used in the present study histologically and ultrastructurally resemble RA lesions [26], with synovial proliferation along the articular surface and subsequent invasion with erosion of the articular cartilage and subchondral bone. Although visual disease scores (ASs) did not show any significant difference between P-NT.II-treated and control (scrambled-P-NT.II-treated or untreated) groups, the results obtained from gross histologic analysis (Table 1) and semiquantitative analysis of pathologic parameters (Fig. 3) clearly demonstrate the beneficial effect of peptide treatment in preventing synovitis, cartilage destruction, and bone erosion. Similar discrepancies between AS and HS have also been reported in TNF-transgenic and other experimental models of arthritis. Redlich and colleagues [27] recently reported a protective effect of osteoprotegerin treatment on bone damage in Tg197 mice, with lack of any beneficial effect on the clinical symptoms. In another experimental model of passive collagen-induced arthritis using JNK2-deficient mice, it has been shown that clinical symptoms appear to be slightly more severe than HS despite significant reductions in joint destruction due to preservation of the articular cartilage [28]. It seems, therefore, that preservation of the bone structure may not always correlate with the clinical symptoms. The striking difference observed in the ultrastructural features of the articular cartilage and synovial membrane in our animal model before and after peptide treatment did confirm that P-NT.II administered as an exogenous drug in this TNF transgenic mouse model of RA was able to improve the overall morphology and the cellular component of the synovium, and of the cartilage in particular.

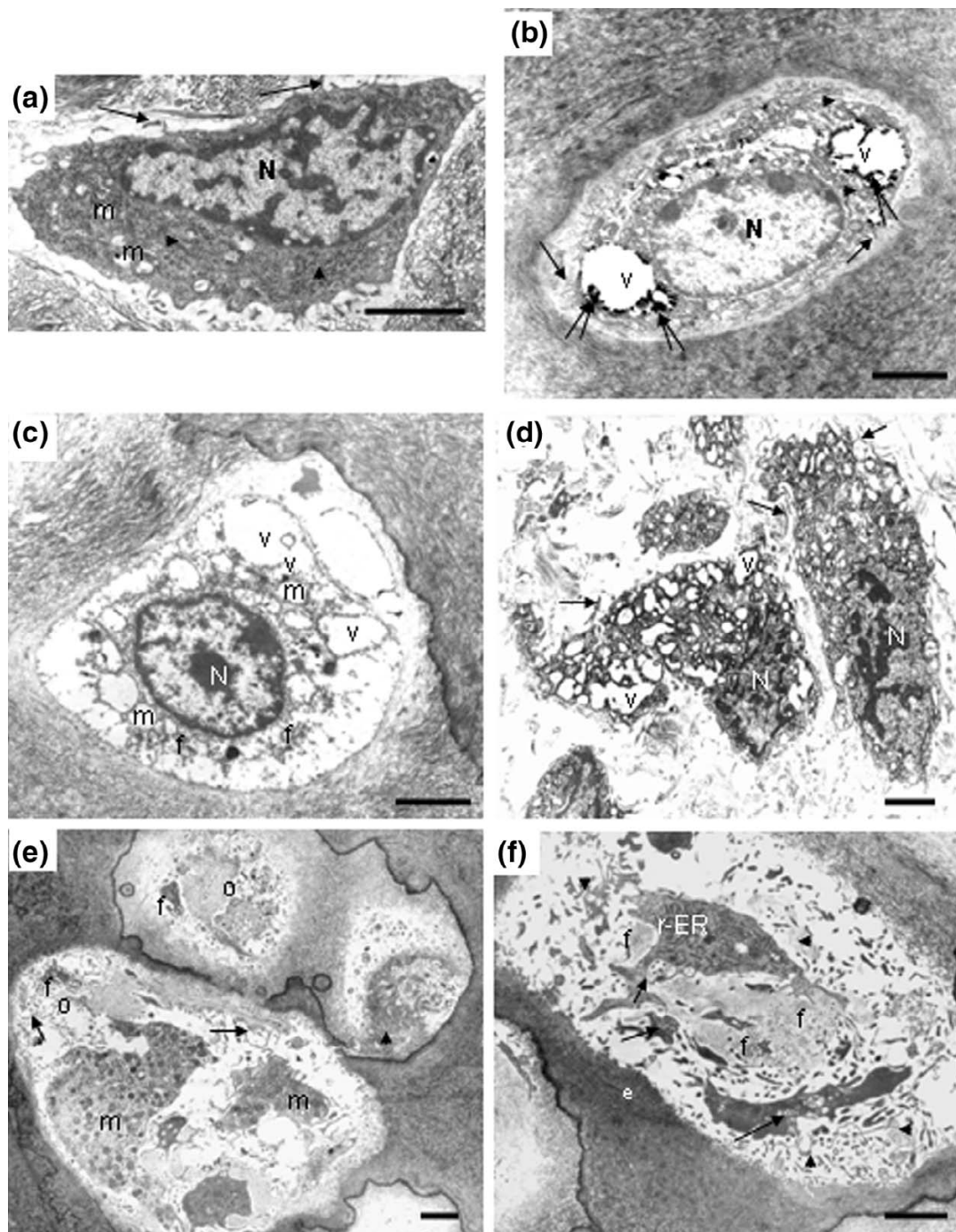
Figure 3

Histopathologic parameters

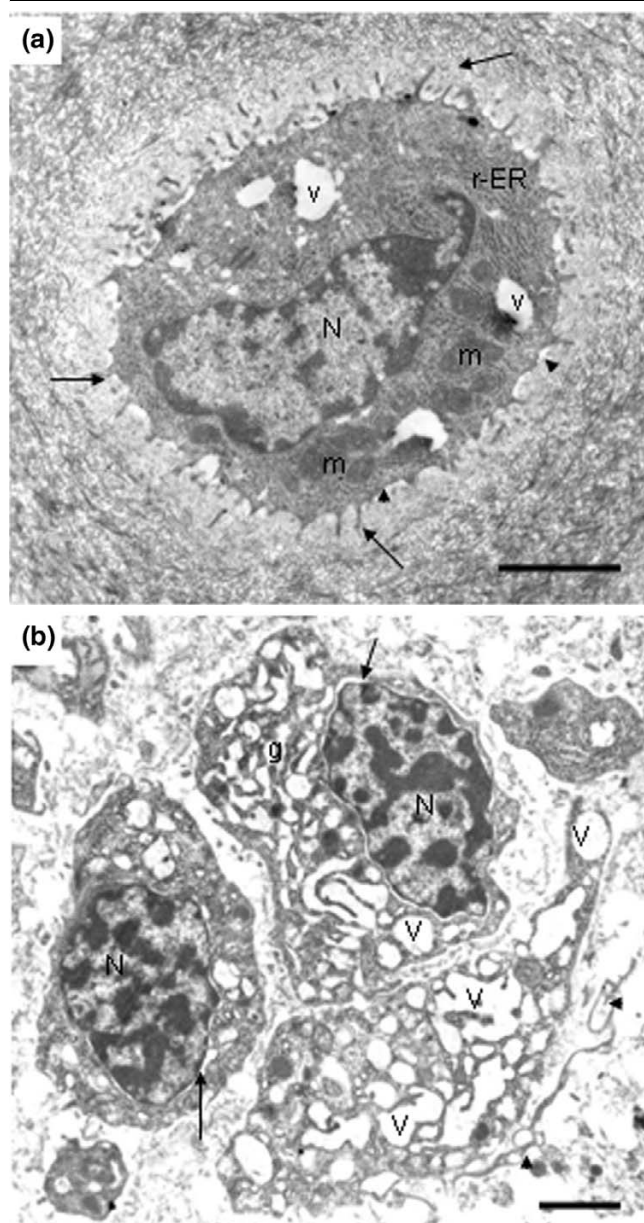
Histopathologic score (HS) analysis of various histopathologic parameters in Tg197 mice. Synovitis, cartilage degradation, and bone erosion were semiquantitatively assessed in the ankle joints of Tg197 mice that were untreated, treated with P-NT.II, or treated with scrambled-P-NT.II ($N = 4/\text{group}$) at 4 weeks post-treatment (i.e. age 8 weeks). The HS indicates a protective effect of P-NT.II in all three histopathologic parameters of arthritis. Statistical analysis revealed a greater beneficial effect of P-NT.II on cartilage destruction and bone erosion (** $P < 0.01$ versus untreated or scrambled-P-NT.II-treated groups for both parameters) than on synovitis (* $P < 0.05$ versus untreated or scrambled-P-NT.II-treated groups).

Ultrastructural changes of ankle articular cartilage and synovium in Tg197 mice were evaluated using transmission electron microscopy, before and during the 4-week course of treatment. Histologically, we observed an apparent suppression of pannus formation and minimal erosive damage to the articular cartilage and subchondral bone. At 1–4 weeks post-treatment with peptide (i.e. at age 5–8 weeks), the number of inflammatory cells in the synovial tissue was reduced as early as 1 week after initiation of treatment, and the structural organization of the synovial membrane of the ankle joint appeared less modified. In the P-NT.II-treated group, lesions such as synovial adhesions, cell fragmentation due to degeneration of synoviocytes, and dilation of the r-ER and distorted cristae of type B cells were less obvious than in the untreated or scrambled-P-NT.II-treated groups. In our cell-culture experiments using mouse macrophages, P-NT.II has been found to dose-dependently inhibit LPS- or TNF-induced PGE_2 production, with a potency equal to that of a potent and selective sPLA₂ inhibitor, LY315920 [29]. It is possible that P-NT.II may modulate ultrastructural modifications to the synovium by reducing the bioavailability of arachidonic acid (AA) through sPLA₂ inhibition, and

Figure 4



Chondrocytes of wild-type controls and untreated Tg197 mice. **(a)** Wild-type control at age 8 weeks: nucleus (N), plasma membrane with short cytoplasmic protrusions (arrow), rough endoplasmic reticulum (r-ER) (arrowhead), and mitochondria (m); **(b)** untreated Tg197 mouse at age 4 weeks: nucleus (N) and plasma membrane with cytoplasmic thin protrusions (arrow) appear normal, while the cytoplasm shows vacuoles (v) with granular materials inside (double arrow) and dilated cisternae (arrowhead). **(c-f)** Untreated Tg197 mouse at age 8 weeks: degenerating chondrocytes showing the following: **(c)** transparent cytoplasm with nucleus (N) and an accumulation of intracytoplasmic filaments (f), vacuoles (v) and mitochondria (m) with distorted cristae; **(d)** greatly vacuolated cytoplasm (v), and pyknotic nuclei (N) with cytoplasmic projections coming apart from the cell (arrow); **(e)** cell organelles from disintegrated cells (o), mitochondria (m), bundles of densely packed collagen fibres (arrowhead), small residues of intermediate filaments (f), and broken cellular processes (arrow); **(f)** swollen and disrupted r-ER, and bundles of thickened intermediate filaments (f). Basement membrane, cytoplasmic organelles (arrow), and cellular processes (arrowhead) were also fragmented. Electron-dense areas (e) are seen in the intercellular matrix. *N* = 4 joints; mean percentage of degenerating chondrocytes = 40% and 80% of total at 4 and 8 weeks of age, respectively. Bars = 2 μ m.

Figure 5

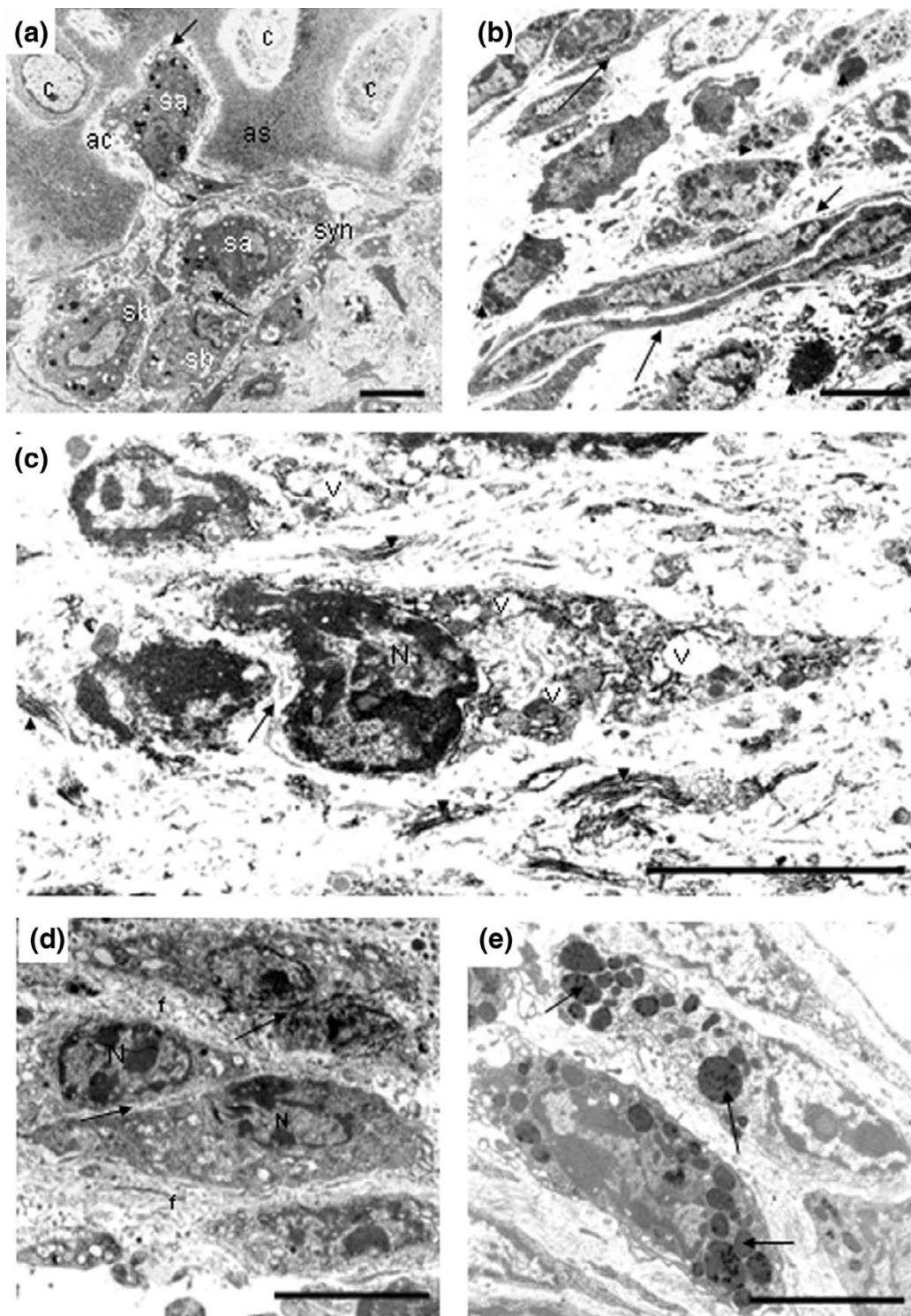
Chondrocytes of treated Tg197 mice. **(a)** Chondrocytes of P-NT.II-treated Tg197 mice at 5–8 weeks of age (i.e. 1–4 weeks post-treatment) were similar to those described for normal chondrocytes, with almost intact nucleus (N), basement membrane (arrowhead), and cytoplasmic organelles – vacuoles (v), rough endoplasmic reticulum (r-ER), mitochondria (m); **(b)** Most chondrocytes of Tg197 mice treated with scrambled P-NT.II at age 8 weeks (i.e. 4 weeks post-treatment) were degenerated, with vacuolated cytoplasm (v), a disrupted Golgi complex (g), pyknotic nuclei (N) with a well-defined, enlarged perinuclear space (arrows), and cytoplasmic projections broken from the cell (arrowhead). $N = 4$ joints/group; mean percentage of degenerating chondrocytes at age 8 weeks = 20% and 75% of total in (a) and (b), respectively. Bars = 2 μ m.

suppress the severity of the prostaglandin-mediated inflammatory response in the synovium.

The ultrastructural features of the articular cartilage observed in this human TNF transgenic mouse model of RA suggest that the chondrocyte may be one of the important targets of the peptide intervention in modulating the progression of the joint erosion. Our extensive histopathologic analysis of joints in the Tg197 TNF model in this study (Fig. 3) has revealed both articular cartilage destruction and subchondral bone erosion at the advanced stages of disease (i.e. 8 weeks of age). Similar severe cartilage destruction in Tg197 mice at 7–8 weeks of age has previously been shown as evidenced by the loss of safranin-O staining [22]. Massive cartilage and subchondral bone erosion in the joints is the hallmark of inflammatory arthritis in the TNF transgenic mouse model [30]. At 3–4 weeks post-treatment (i.e. at 7–8 weeks of age), P-NT.II significantly reduced chondrocyte necrobiosis, which was frequently seen in the proximity of invading synovium in untreated controls at same age. It is possible that sPLA₂ might be involved in cartilage destruction in the TNF-transgenic mouse model. sPLA₂ found in the synovial fluid has been reported to originate from chondrocytes and not from the synovial lining or inflammatory cells [31]. Human articular chondrocytes synthesize and constitutively release sPLA₂, and are therefore suggested to be responsible for the high concentration of sPLA₂ present in articular cartilage [32]. cPLA₂ is also reported to be involved in PGE₂ production by osteoblast cells [33], while there are reports indicating that sPLA₂ augments cPLA₂ expression in mouse osteoblasts via endogenous PGE [13,34]. Because of the significant functional coupling and/or synergism that can exist between cPLA₂ and sPLA₂ in various cells [3,13,33-35], sPLA₂ could conceivably be involved in chondrocyte destruction in RA by playing a role in bone resorption through crosstalk with cPLA₂.

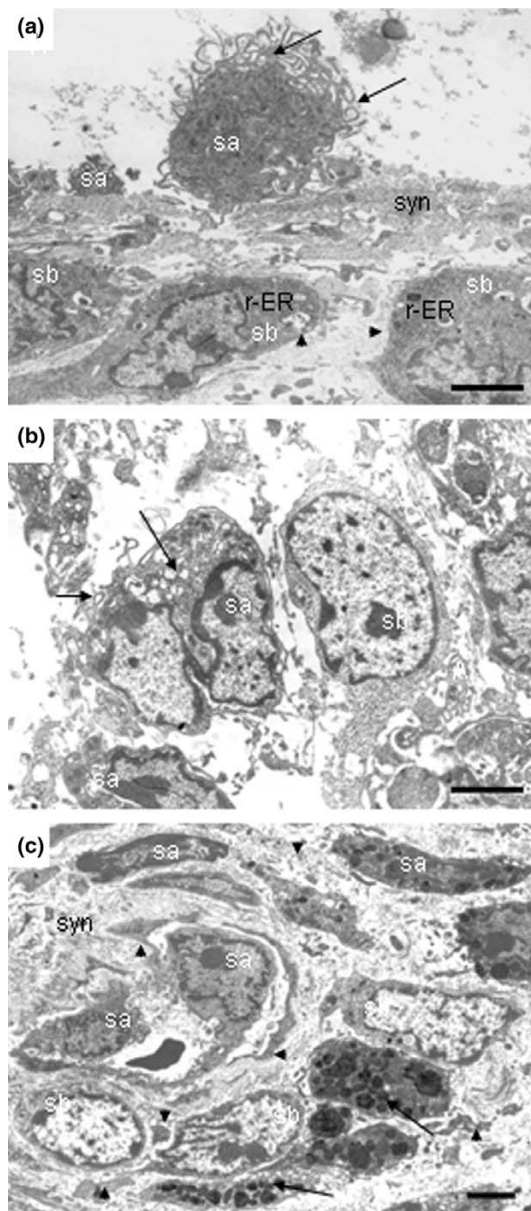
We have found significantly elevated levels of circulating sPLA₂ in Tg197 mice at 8 weeks of age as compared with the much lower baseline levels detected at 4 weeks of age. Elevated levels of sPLA₂ have been reported in the plasma of patients with acute and chronic inflammatory diseases [36]. sPLA₂ can mobilize AA to induce the *de novo* synthesis of eicosanoids in a variety of inflammatory cells [37], leading to subsequent release of proinflammatory mediators. Recently, sPLA₂ has been shown to amplify TNF-induced PGE₂ synthesis in human rheumatoid synoviocytes [8], a process that is blocked by cyclic peptide inhibitors of human sPLA₂ [38]. The use of a low-molecular-weight peptide, such as P-NT.II, that effectively lowers sPLA₂ could be of clear clinical benefit in similar situations. Our results obtained with P-NT.II-treated Tg197 mice demonstrated that this new peptide inhibitor significantly suppressed the circulating sPLA₂ activity in those mice, whereas scrambled P-NT.II (negative control peptide) was without any effect.

Figure 6



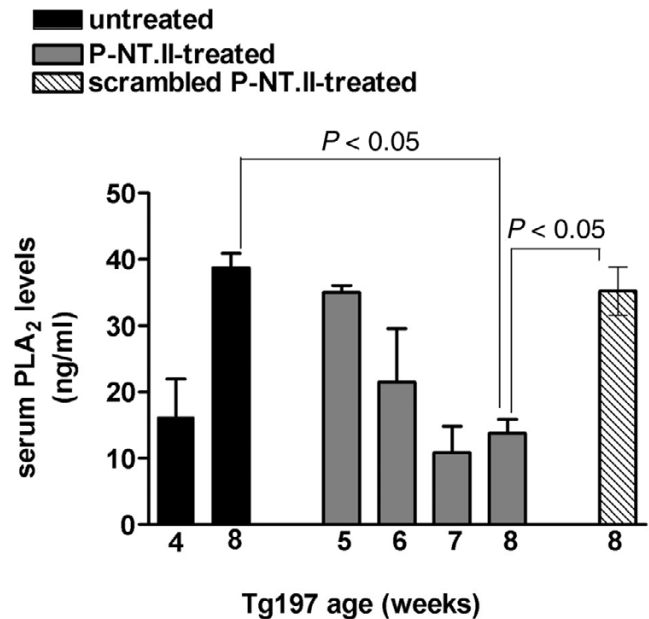
Synovium of untreated Tg197 mice at age 8 weeks. **(a)** Proliferation of the synovial tissue (syn) in the articular cavity (ac) showing macrophage-like type A synoviocytes (sa) with thin cytoplasmic protrusions (arrow) invading the articular surface (as), and closely packed secretory type B synoviocytes (sb) seen in the superficial layer of pannus. **(b)** The synovial membrane was lined by closely packed, elongated (arrow) or rounded synoviocytes with infiltrating cells (arrowhead) present under the synovium. **(c)** Degenerating synoviocyte with disintegrated nuclei (arrow) and vacuolated (v) cytoplasm along with disrupted collagen fibres (arrowhead) randomly seen in the synovium. **(d)** Adherent-type junction (arrow) sealing two synoviocytes with fibrin (f) between them. **(e)** Synoviocytes appeared flattened, and partially degenerated mast cells (arrow) are seen under the synovium. *N* = 4 joints; mean percentage of degenerating synoviocytes = 80% of total cells. Bars = 5 μ m. c, chondrocytes; N, nucleus.

Figure 7



Synovium of treated Tg197 mice. **(a)** Nontransgenic wild-type group (control) at age 8 weeks: type A (sa) and type B (sb) synoviocytes are arranged loosely in the synovium (syn). Type A cells are characterized by many thin filopodia (arrow), while type B cells contain many instances of rough endoplasmic reticulum (r-ER), small vesicles, and basement membrane structures (arrowhead); **(b)** P-NT.II-treated Tg197 group at 5-8 weeks of age: synoviocyte A cells (sa) with characteristic cytoplasmic processes intermingled with those of neighboring cells (arrow) and B cells (sb), seen at age 6-8 weeks of age (i.e. 2-4 weeks post-treatment), appear unmodified during the time course (1-4 weeks) of treatment. The ultrastructural features are similar to those seen in the ankle joints of wild-type controls in (a). **(c)** Scrambled-P-NT.II-treated Tg197 group at age 8 weeks: type A (sa) and B (sb) synovial cells were seen lining up close together, and many cell fragments (arrowheads) resulting from fibrous degeneration of endothelial cells were present in the synovium (syn), along with infiltrating mast cells (arrows). $N = 4$ joints/group; mean percentage of degenerating synoviocytes = 24% and 75% of total in (b) and (c), respectively. Bars = 2 μm .

Figure 8



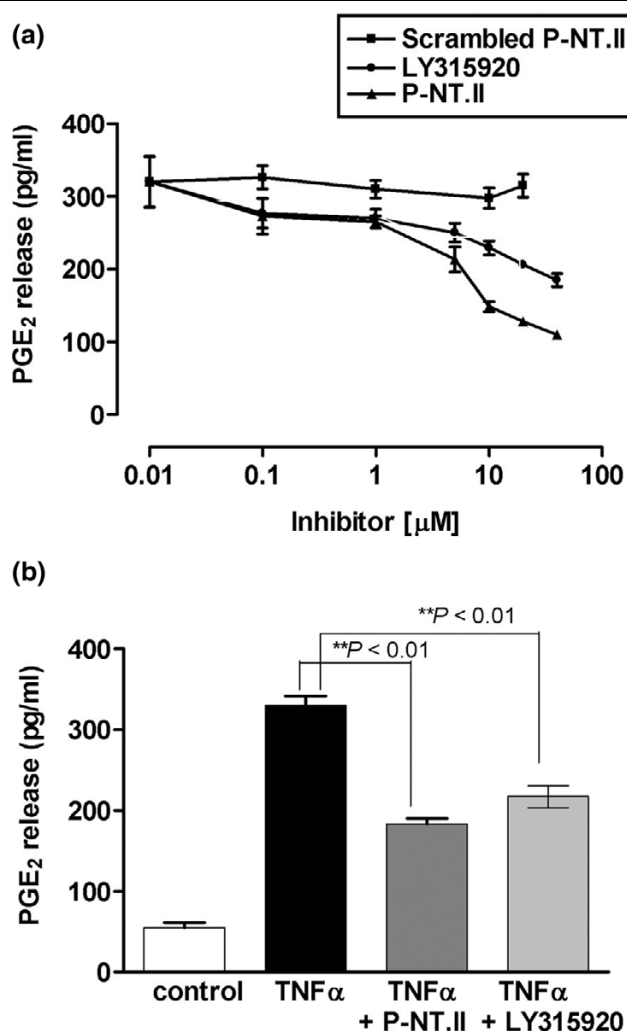
Time course of serum phospholipase A_2 (sPLA $_2$) levels. Serum sPLA $_2$ levels were measured with an *Escherichia coli* membrane assay in blood samples collected from untreated, P-NT.II-treated, and scrambled-P-NT.II-treated Tg197 mice at weekly intervals during the 4 weeks' time course of treatment. Values are the mean \pm SD ($N = 4$ /group). One-way ANOVA with Bonferroni's multiple comparison post test: $P < 0.05$, untreated versus P-NT.II-treated (age 8 weeks); $P < 0.05$, scrambled-P-NT.II-treated versus P-NT.II-treated (age 8 weeks).

The data obtained from the present study suggest that P-NT.II ameliorates synovitis and bone and cartilage erosions in the joints through modulation of circulatory and localized sPLA $_2$, which might otherwise amplify TNF-dependent pathways in rheumatoid synovium. Although the mode of action of sPLA $_2$ in this animal model is not exactly known, the potential mechanism may involve binding to a receptor [39], followed by internalization [40] and transfer of sPLA $_2$ to intracellular pools of phospholipids enriched in AA [41]. Further catalysis by sPLA $_2$ through surface interactions can then initiate and promote pathology by releasing AA, which can subsequently be converted to proinflammatory prostaglandins and leukotrienes. There are no published reports of sPLA $_2$ inhibitors showing benefit on bone erosion. The ultrastructural evidence of the beneficial effect of the peptide on joint destruction as shown here suggests a possible use of sPLA $_2$ inhibitors in the treatment of inflammatory bone loss diseases such as RA. However, some caution is advisable in the interpretation of the findings, since the nature of the arthritis in a purely TNF-driven disease, such as that observed in TNF transgenic mice, may not truly reflect the situation in human inflammatory joint diseases.

Conclusion

The present study provides ultrastructural demonstration of the modulatory effect of the P-NT.II peptide on synovial

Figure 9



Modulation of lipopolysaccharide (LPS)- and tumor necrosis factor (TNF)-stimulated PGE₂ release. Macrophages (5×10^5 cells/ml) from subcultured J774 mouse cell line were incubated with (a) LPS (2 µg/ml) or (b) TNF (10 ng/ml) in the absence or the presence of various concentrations (0–40 µM) of P-NT.II, LY315920, or scrambled P-NT.II for 20 hours. Supernatants were collected, and PGE₂ release in the medium was determined by enzyme-linked immunosorbent assay. Results are shown as the mean \pm SEM of five experiments performed in duplicate. $**P < 0.01$ between inhibitor-treated and untreated cultures.

inflammation and joint destruction in TNF-driven Tg197 mouse model of human RA. The results suggest that sPLA₂ seems to play a significant role in inflammatory arthritis, and sPLA₂ inhibitors may be useful for the development of novel agents to treat RA and other inflammatory diseases.

Competing interests

None declared.

Acknowledgements

We are grateful to Mr Spiros Lalos and Ms Alexia Giannakopoulou, Institute of Immunology, Biomedical Sciences Research Centre, Al Fleming, Greece, and Ms Ng Geok Lan and Ms Chan Yee Gek, Department of

Anatomy, Faculty of Medicine, National University of Singapore, for their excellent technical assistance.

References

- Nevalainen TJ, Haapamaki MM, Gronroos JM: **Roles of secretory phospholipases A(2) in inflammatory diseases and trauma.** *Biochim Biophys Acta* 2000, **1488**:83-90.
- Lin MK, Farewell V, Vadas P, Bookman AA, Keystone EC, Pruzanski W: **Secretory phospholipase A2 as an index of disease activity in rheumatoid arthritis. Prospective double blind study of 212 patients.** *J Rheumatol* 1996, **23**:1162-1166.
- Huwiler A, Staudt G, Kramer RM, Pfeilschifter J: **Cross-talk between secretory phospholipase A2 and cytosolic phospholipase A2 in rat renal mesangial cells.** *Biochim Biophys Acta* 1997, **1348**:257-272.
- Jamal OS, Conaghan PG, Cunningham AM, Brooks PM, Munro VF, Scott KF: **Increased expression of human type IIa secretory phospholipase A2 antigen in arthritic synovium.** *Ann Rheum Dis* 1998, **57**:550-558.
- Vadas P, Pruzanski W, Kim J, Fox N: **The proinflammatory effect of intra-articular injection of soluble human and venom phospholipase A2.** *Am J Pathol* 1989, **134**:807-811.
- Bomalaski JS, Lawton P, Browning JL: **Human extracellular recombinant phospholipase A2 induces an inflammatory response in rabbit joints.** *J Immunol* 1991, **146**:3904-3910.
- Lin MK, Katz A, van den BH, Kennedy B, Stefanski E, Vadas P, Pruzanski W: **Induction of secretory phospholipase A2 confirms the systemic inflammatory nature of adjuvant arthritis.** *Inflammation* 1998, **22**:161-173.
- Bidgood MJ, Jamal OS, Cunningham AM, Brooks PM, Scott KF: **Type IIA secretory phospholipase A2 up-regulates cyclooxygenase-2 and amplifies cytokine-mediated prostaglandin production in human rheumatoid synoviocytes.** *J Immunol* 2000, **165**:2790-2797.
- Feldmann M: **What is the mechanism of action of anti-tumour necrosis factor-alpha antibody in rheumatoid arthritis?** *Int Arch Allergy Immunol* 1996, **111**:362-365.
- Akira S, Kishimoto T: **IL-6 and NF-IL6 in acute-phase response and viral infection.** *Immunol Rev* 1992, **127**:25-50.
- Papadakis KA, Targan SR: **Tumor necrosis factor: biology and therapeutic inhibitors.** *Gastroenterology* 2000, **119**:1148-1157.
- Triggiani M, Granata F, Oriente A, Gentile M, Petraroli A, Balestrieri B, Marone G: **Secretory phospholipases A2 induce cytokine release from blood and synovial fluid monocytes.** *Eur J Immunol* 2002, **32**:67-76.
- Murakami M, Kuwata H, Amakasu Y, Shimbara S, Nakatani Y, Atsumi G, Kudo I: **Prostaglandin E2 amplifies cytosolic phospholipase A2- and cyclooxygenase-2-dependent delayed prostaglandin E2 generation in mouse osteoblastic cells. Enhancement by secretory phospholipase A2.** *J Biol Chem* 1997, **272**:19891-19897.
- Schrier DJ, Flory CM, Finkel M, Kuchera SL, Lesch ME, Jacobson PB: **The effects of the phospholipase A2 inhibitor, manolide, on cartilage degradation, stromelysin expression, and synovial fluid cell count induced by intraarticular injection of human recombinant interleukin-1 alpha in the rabbit.** *Arthritis Rheum* 1996, **39**:1292-1299.
- Garcia-Pastor P, Randazzo A, Gomez-Paloma L, Alcaraz MJ, Paya M: **Effects of petrosaspongiolide M, a novel phospholipase A2 inhibitor, on acute and chronic inflammation.** *J Pharmacol Exp Ther* 1999, **289**:166-172.
- Miele L: **Antiflammins. Bioactive peptides derived from uteroglobin.** *Ann N Y Acad Sci* 2000, **923**:128-140.
- Thwin MM, Gopalakrishnakone P, Kini RM, Armugam A, Jeyaseelan K: **Recombinant antitoxic and antiinflammatory factor from the nonvenomous snake Python reticulatus: phospholipase A2 inhibition and venom neutralizing potential.** *Biochemistry* 2000, **39**:9604-9611.
- Thwin MM, Satish RL, Chan ST, Gopalakrishnakone P: **Functional site of endogenous phospholipase A2 inhibitor from python serum.** *Eur J Biochem* 2002, **269**:719-727.
- Thwin MM, Ong WY, Fong CW, Sato K, Kodama K, Farooqui AA, Gopalakrishnakone P: **Secretory phospholipase A2 activity in the normal and kainate injected rat brain, and inhibition by a**

- peptide derived from python serum. *Exp Brain Res* 2003, **150**:427-433.
20. Keffer J, Probert L, Cazlaris H, Georgopoulos S, Kaslaris E, Kioussis D, Kollias G: **Transgenic mice expressing human tumour necrosis factor: a predictive genetic model of arthritis.** *EMBO J* 1991, **10**:4025-4031.
 21. Wooley PH: **Collagen-induced arthritis in the mouse.** *Methods Enzymol* 1988, **162**:361-373.
 22. Douni E, Sfrikakis PP, Haralambous S, Fernandes P, Kollias G: **Attenuation of inflammatory polyarthritis in TNF transgenic mice by diacerein: comparative analysis with dexamethasone, methotrexate and anti-TNF protocols.** *Arthritis Res Ther* 2004, **6**:R65-R72.
 23. Arsenault AL, Lhotak S, Hunter WL, Banquerigo ML, Brahn E: **Taxol (paclitaxel) involution of articular cartilage destruction in collagen induced arthritis: an ultrastructural demonstration of an increased superficial chondroprotective layer.** *J Rheumatol* 2000, **27**:582-588.
 24. Henzgen S, Petrow PK, Thoss K, Brauer R: **Degradation of articular cartilage during the progression of antigen-induced arthritis in mice. A scanning and transmission electron microscopic study.** *Exp Toxicol Pathol* 1996, **48**:255-263.
 25. Lapadula G, Nico B, Cantatore FP, La Canna R, Roncali L, Pipitone V: **Early ultrastructural changes of articular cartilage and synovial membrane in experimental vitamin A-induced osteoarthritis.** *J Rheumatol* 1995, **22**:1913-1921.
 26. Ghadially FN: *Fine structure of the synovial joints. A text and atlas of the ultrastructure of normal and pathological articular tissues* London: Butterworth; 1983.
 27. Redlich K, Hayer S, Maier A, Dunstan CR, Tohidast-Akrad M, Lang S, Turk B, Pietschmann P, Woloszczuk W, Haralambous S, Kollias G, Steiner G, Smolen JS, Schett G: **Tumor necrosis factor alpha-mediated joint destruction is inhibited by targeting osteoclasts with osteoprotegerin.** *Arthritis Rheum* 2002, **46**:785-792.
 28. Han Z, Chang L, Yamanishi Y, Karin M, Firestein GS: **Joint damage and inflammation in c-Jun N-terminal kinase 2 knockout mice with passive murine collagen-induced arthritis.** *Arthritis Rheum* 2002, **46**:818-823.
 29. Snyder DW, Bach NJ, Dillard RD, Draheim SE, Carlson DG, Fox N, Roehm NW, Armstrong CT, Chang CH, Hartley LW, Johnson LM, Roman CR, Smith AC, Song M, Fleisch JH: **Pharmacology of LY315920/S-5920, [[3-(aminooxoacetyl)-2-ethyl-1-(phenylmethyl)-1H-indol-4-yl]oxy] acetate, a potent and selective secretory phospholipase A2 inhibitor: A new class of anti-inflammatory drugs, SPL.** *J Pharmacol Exp Ther* 1999, **288**:1117-1124.
 30. Li P, Schwarz EM: **The TNF-alpha transgenic mouse model of inflammatory arthritis.** *Springer Semin Immunopathol* 2003, **25**:19-33.
 31. Nevalainen TJ, Marki F, Kortesoja PT, Grutter MG, Di Marco S, Schmitz A: **Synovial type (group II) phospholipase A2 in cartilage.** *J Rheumatol* 1993, **20**:325-330.
 32. Pruzanski W, Bogoch E, Katz A, Wloch M, Stefanski E, Grouix B, Sakotic G, Vadas P: **Induction of release of secretory nonpancreatic phospholipase A2 from human articular chondrocytes.** *J Rheumatol* 1995, **22**:2114-2119.
 33. Miyaoura C, Inada M, Matsumoto C, Ohshiba T, Uozumi N, Shimizu T, Ito A: **An essential role of cytosolic phospholipase A2alpha in prostaglandin E2-mediated bone resorption associated with inflammation.** *J Exp Med* 2003, **197**:1303-1310.
 34. Kudo I, Murakami M: **Diverse functional coupling of prostanoid biosynthetic enzymes in various cell types.** *Adv Exp Med Biol* 1999, **469**:29-35.
 35. Balsinde J, Balboa MA, Insel PA, Dennis EA: **Regulation and inhibition of phospholipase A2.** *Annu Rev Pharmacol Toxicol* 1999, **39**:175-189.
 36. Vadas P: **Elevated plasma phospholipase A2 levels: correlation with the hemodynamic and pulmonary changes in gram-negative septic shock.** *J Lab Clin Med* 1984, **104**:873-881.
 37. Mayer RJ, Marshall LA: **New insights on mammalian phospholipase A2(s); comparison of arachidonoyl-selective and -nonselective enzymes.** *FASEB J* 1993, **7**:339-348.
 38. Church WB, Inglis AS, Tseng A, Duell R, Lei PW, Bryant KJ, Scott KF: **A novel approach to the design of inhibitors of human secreted phospholipase A2 based on native peptide inhibition.** *J Biol Chem* 2001, **276**:33156-33164.
 39. Lambeau G, Lazdunski M: **Receptors for a growing family of secreted phospholipases A2.** *Trends Pharmacol Sci* 1999, **20**:162-170.
 40. Murakami M, Koduri RS, Enomoto A, Shimbara S, Seki M, Yoshihara K, Singer A, Valentin E, Ghomashchi F, Lambeau G, Gelb MH, Kudo I: **Distinct arachidonate-releasing functions of mammalian secreted phospholipase A2s in human embryonic kidney 293 and rat mastocytoma RBL-2H3 cells through heparan sulfate shuttling and external plasma membrane mechanisms.** *J Biol Chem* 2001, **276**:10083-10096.
 41. Granata F, Balestrieri B, Petraroli A, Giannattasio G, Marone G, Triggiani M: **Secretory phospholipases A2 as multivalent mediators of inflammatory and allergic disorders.** *Int Arch Allergy Immunol* 2003, **131**:153-163.